Supplementary Figures

Compartmentalized nonsense-mediated mRNA decay regulates synaptic plasticity and cognitive function via GluR1 signaling

Michael Notaras[1], Megan Allen[1], Francesco Longo[2], Nicole Volk[1], Miklos Toth[3], Noo Li Jeon[4], Eric Klann[2], Dilek Colak[1,5,*]

[1] Center for Neurogenetics, Feil Family Brain and Mind Research Institute, Weill Cornell Medical College, Cornell University, New York City, New York, USA.
[2] Center for Neural Science, New York University, New York City, New York, USA.
[3] Department of Pharmacology, Weill Cornell Medical College, Cornell University, New York City, New York, USA.
[4] School of Mechanical and Aerospace Engineering, Seoul National University, Seoul, South Korea.
[5] Gale & Ira Drukier Institute for Children's Health, Weill Cornell Medical College, Cornell University, New York City, New York, USA.

*Correspondence: dic2009@med.cornell.edu

Figure S1.

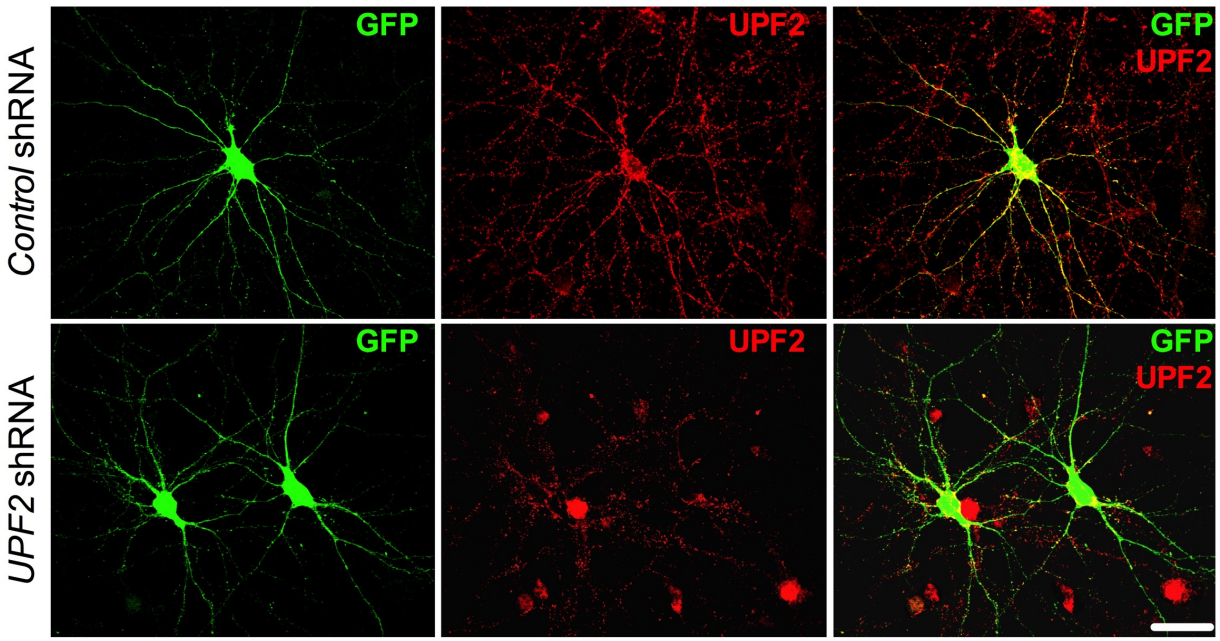

Fig. S1 | Knockdown of UPF2 in mouse hippocampal neurons by *UPF2*-shRNA:GFP lentivirus.
To disrupt NMD, we targeted the *UPF2* mRNA using *UPF2*-shRNA:GFP lentivirus. Canonical NMD is completed by the interaction of UPF1, UPF2 and UPF3 proteins. While UPF1 function is not restricted to the NMD pathway [1], UPF2 has been successfully used to disrupt NMD in several studies [2-4]. We infected E16 hippocampal neurons at DIV7 with *control*- or *UPF2*-shRNA virus. To assess the knockdown of UPF2, we fixed the cells at DIV14 and performed immunohistochemistry for UPF2. *UPF2*-shRNA application resulted in a robust depletion of UPF2 within infected neurons and their dendrites, while UPF2 expression remained intact in scrambled *control*-shRNA cultures and non-infected neurons in *UPF2*-shRNA cultures (UPF2+, GFP- cells in *UPF2*-shRNA panel). In Figures 1-6, we depleted UPF2 using this *UPF2*-shRNA:GFP lentivirus. Scale bar: 30 μm.

Figure S2.

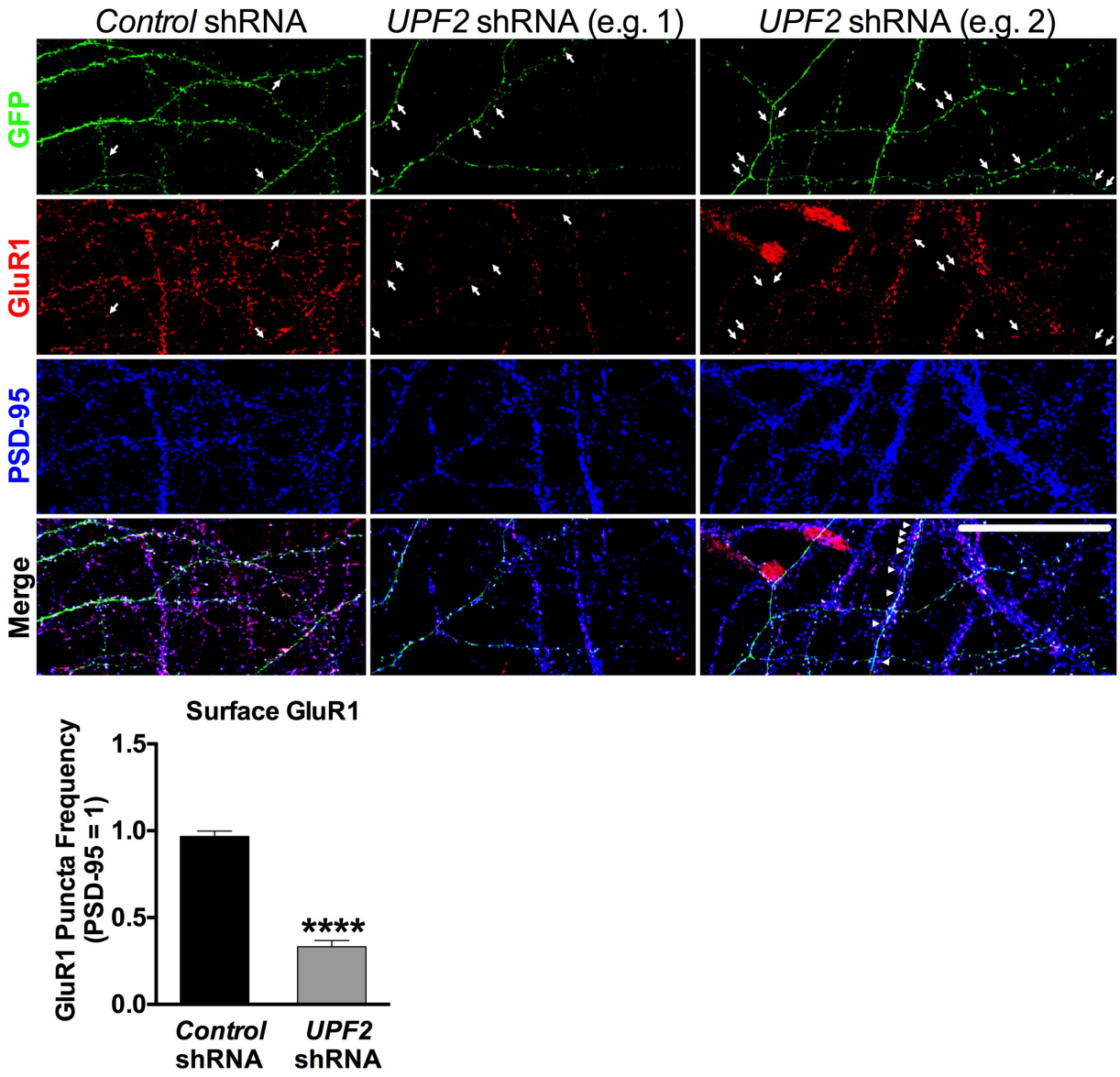
Control shRNA
UPF2 shRNA (e.g. 1)
UPF2 shRNA (e.g. 2)
GFP
GluR1
PSD-95
Merge
Surface GluR1
GluR1 Puncta Frequency (PSD-95 = 1)
1.5
1.0
0.5
0.0
****
Control shRNA
UPF2 shRNA

Fig. S2 | Decrease in GluR1 surface levels in NMD-deficient dendrites was also recapitulated when the synaptic marker PSD-95, in addition to synapsin, was used for quantifications.

In Figure 1, we show that knockdown of UPF2 in hippocampal neurons led to a robust depletion of surface GluR1 levels without altering the mRNA transcription of this receptor. For these quantifications, we used synapsin as a normalization marker as is consistent with prior work (see Methods). To address whether this GluR1 phenotype is recapitulated when another synaptic marker is used for normalization, we repeated this experiment using the postsynaptic marker PSD-95. Similar to the synapsin quantifications, the ablation of UPF2 in hippocampal neurons resulted in a significant depletion of surface GluR1 levels when synapses were identified and normalized against PSD-95 expression (n=3 biological replicates per group; 11 dendrites from 7 neurons for *control*-shRNA cultures, and 12 dendrites from 8 neurons for *UPF2*-shRNA cultures). Arrows show examples of GFP and GluR1 colocalization in spines. Two panels of *UPF2*-shRNA dendrites are presented to exemplify contrasting aspects of GluR1 expression. Arrows depict the loss of surface GluR1 in spines of *UPF2*-shRNA infected hippocampal neurons relative to control cultures. Arrowheads in the merged panel of *UPF2*-shRNA example 2 depict a non-infected dendrite segment with intact GluR1 expression that is overlapping an infected dendrite that exhibits reduced GluR1 colocalization in isolated GFP+ spines. These data replicate the depletion of GluR1 surface levels in NMD-deficient dendrites presented in Figure 1, and provide confirmation that synapsin produces concordant data to PSD-95 when used to evaluate surface GluR1 levels.

Data are represented as mean ± Standard Error of the Mean (SEM); ****$p < 0.0001$. Scale bar: 30 μm.

Figure S3.

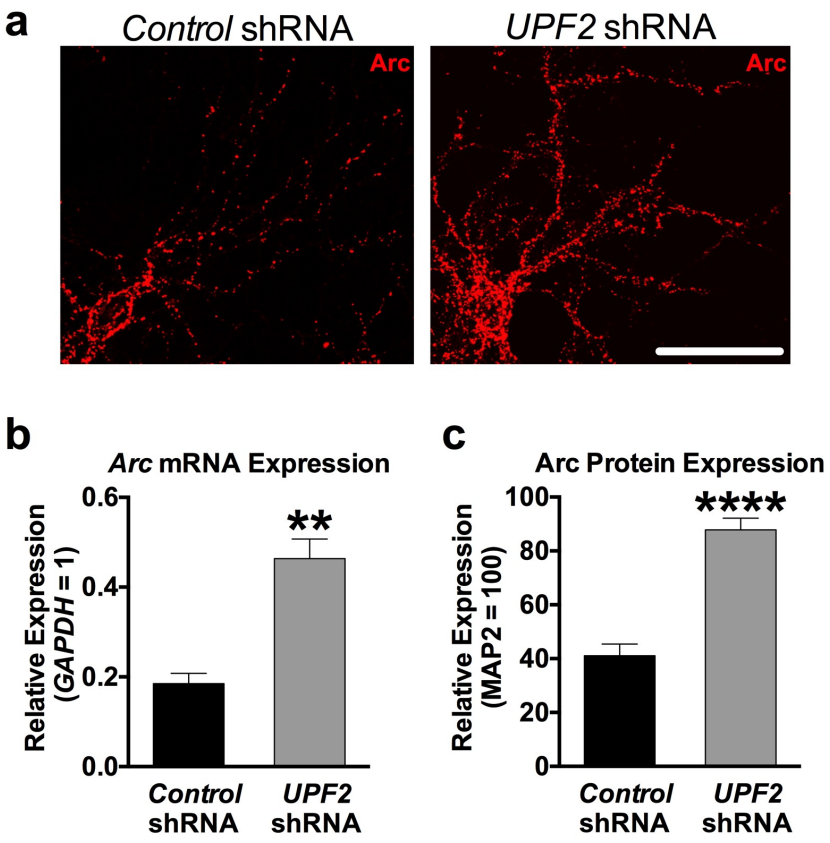
a
Control shRNA
UPF2 shRNA
Arc
Arc
b
Arc mRNA Expression
Relative Expression
(GAPDH = 1)
0.6
0.4
0.2
0.0
**
Control
shRNA
UPF2
shRNA
c
Arc Protein Expression
Relative Expression
(MAP2 = 100)
100
80
60
40
20
0
****
Control
shRNA
UPF2
shRNA

Fig. S3 | Arc levels are increased upon disruption of NMD in hippocampal neurons.

a, Arc immunostaining in mouse hippocampal neurons upon knockdown of UPF2. Disruption of NMD caused a significant reduction in the surface levels of GluR1 without affecting the *GluR1* mRNA levels (Figure 1). This suggests that NMD regulates GluR1 surface expression through other mechanisms than transcription or *GluR1* degradation. GluR1 signaling is modulated by dynamic insertion and removal of the GluR1 receptor to the synaptic surface [5]. The synaptic plasticity protein Arc drives the removal of GluR1 from the surface of synapses. *Arc* mRNA is a known target of NMD. Both *Arc* mRNA and Arc protein are increased in the absence of NMD [2, 6] suggesting that elevated Arc levels may account for the reduced surface expression of GluR1. To confirm that ablation of NMD disrupts endogenous Arc levels, we cultured E16 mouse hippocampal neurons and infected with *control-* or *UPF2*-shRNA lentivirus at DIV7 to disrupt NMD. At DIV21, we performed immunostaining for Arc protein.

b, Quantitative RT-PCR analysis of *Arc* mRNA in NMD-deficient neurons. To quantify *Arc* mRNA, we performed qRT-PCR. *GAPDH* was used as a control transcript. Expression of *Arc* was presented relative to *GAPDH*. Neurons infected with *UPF2*-shRNA lentivirus displayed exaggerated *Arc* mRNA expression (n=3 biological replicates per group) compared to control neurons.

c, Quantifications of Arc protein in NMD-deficient neurons. Quantifications of fluorescent intensity, normalized to MAP2, showed that Arc protein levels are also increased in neurons with disrupted NMD (per group, n=10 dendrites for analysis of fluorescent intensity). Together, these data confirm that Arc levels are increased in the absence of NMD, which likely influences the GluR1 internalization in NMD-deficient dendrites (see Figure 2**a**).

Data are represented as mean ± Standard Error of the Mean (SEM); ** $p < 0.01$, **** $p < 0.0001$. Scale bar: 30 μm.

Figure S4.

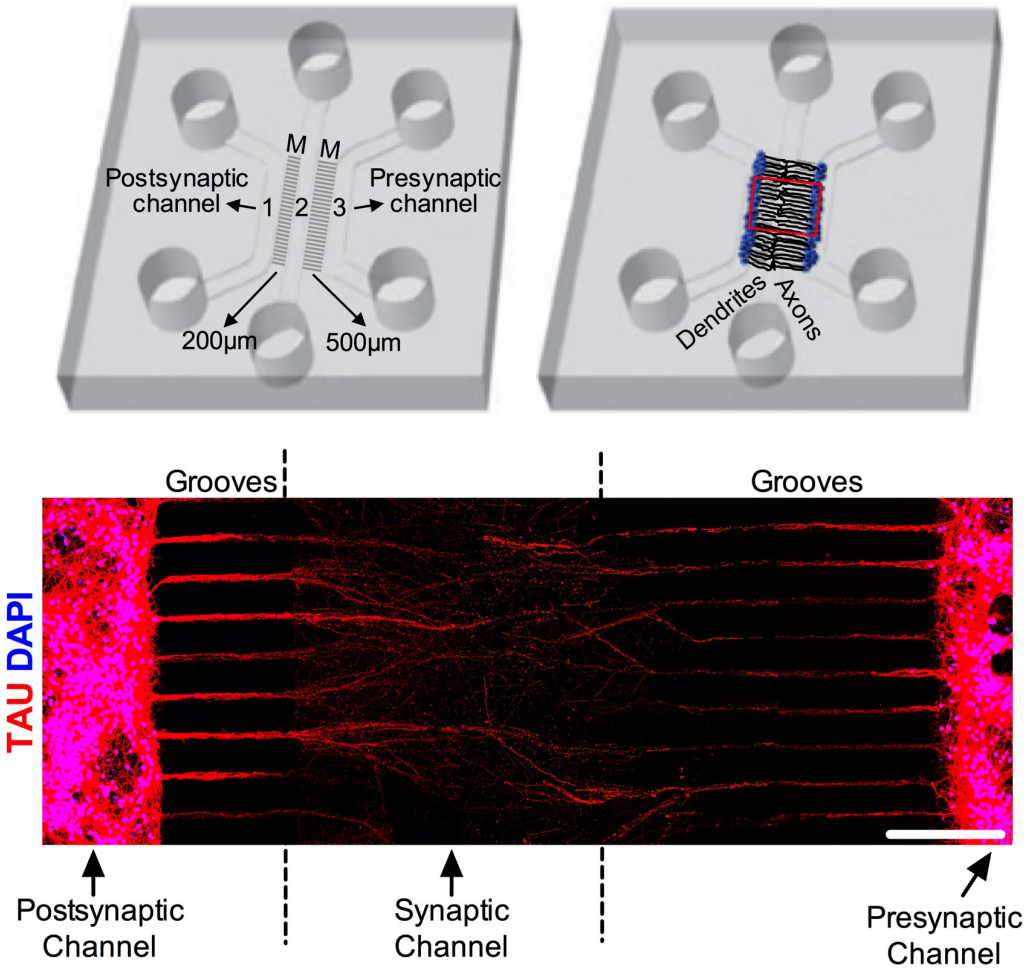
M M
Postsynaptic channel
1 2 3
Presynaptic channel
200µm
500µm
Dendrites
Axons
Grooves
Grooves
TAU DAPI
Postsynaptic Channel
Synaptic Channel
Presynaptic Channel

Fig. S4 | Axonal penetrance of microgrooves in the tripartite microfluidic device. As shown in the schematic presented here, and the MAP2 immunostaining presented in Figure 3, our custom-engineered tripartite microfluidic device only permits the dendrites of neurons from left channel to penetrate the middle channel, which is referred to as synaptic channel. Here, TAU staining shows that axons from both channels extend to the synaptic channel suggesting that axons of both channel 1 and channel 3 can form synapses with dendrites that originated from channel 1. However, due to the limited length, dendrites remain in very close proximity to channel 1 (Figure 3) restricting the dendrite-axon synapses to the proximity to the channel 1. Because axons are very long, and the short microgrooves that separate channel 1 and synaptic channel are just 200 μm in length, the majority of channel 1 axons span the entire synaptic channel and reach channel 3. Thus, the majority of the synapses formed in the synaptic channel consist of dendrites projecting from channel 1 and axons originating from channel 3. UPF2 is not expressed in mature axons (Figure 5), and only dendrites from neurons plated in channel 1 can reach the synaptic channel (Figure 3). Therefore, regardless of where the presynaptic axons project from, or where synapses are formed within the synaptic channel, the manipulation of NMD exclusively in channel 1 is confined to postsynaptic dendrites
Scale bar: 200 μm.

Figure S5.

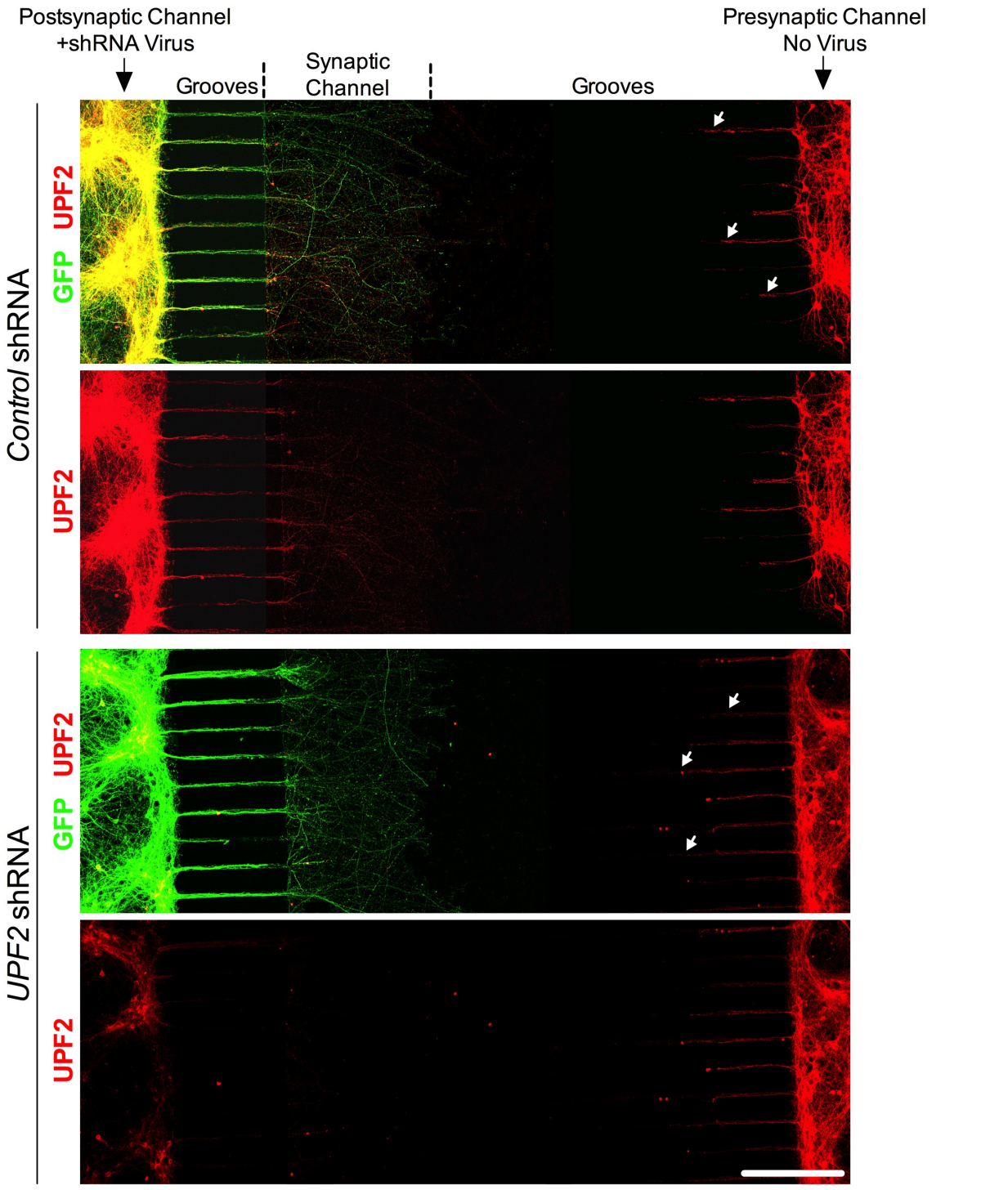
Postsynaptic Channel
+shRNA Virus
Grooves
Synaptic
Channel
Grooves
Presynaptic Channel
No Virus
Control shRNA
GFP UPF2
UPF2
UPF2 shRNA
GFP UPF2
UPF2

Fig. S5 Application of *UPF2* shRNA virus exclusively to the postsynaptic channel results in loss of UPF2 in this channel as well as in dendrites within the synaptic channel but not in presynaptic channel neurons or their projections.
The physical and fluidic isolation of channels is a fundamental feature and component of microfluidic devices, as it permits the selective manipulation/isolation of neuronal populations and compartments. To address the role of NMD in dendrites in synaptic function, we selectively treated postsynaptic channels with *UPF2*-shRNA virus at DIV7. To determine whether the virus application resulted in selective loss of UPF2, we performed immunostainings for UPF2 following fixation of cells at DIV13. Consistent with the fluidic isolation of channels, the GFP signal was specific to infected neurons restricted to the postsynaptic channels and their neurites in the synaptic channel. Selective application of the *UPF2*-shRNA virus in the postsynaptic channel resulted in nearly complete loss of UPF2 protein in this channel, as well as in the dendrites in the synaptic channel, but not in the presynaptic channel. Because mature axons do not express UPF2 (Figure 5), the UPF2-positive signal in the synaptic channels in the control experiment solely reflects dendritic expression. Consistent with this, dendrites that emerged from the presynaptic channel, which only traveled half way through microgrooves (white arrows), also retained their UPF2 expression in both the *control*- and *UPF2*-shRNA experiments (see Figure 3 and Figure S4 for the comparison of dendrite and axon projection in these grooves). In all experiments that employed *control*- or *UPF2*-shRNAs in tripartite devices, viruses were only applied to the postsynaptic cell body channel of microfluidic devices. Scale bar: 200 μm.

Figure S6.

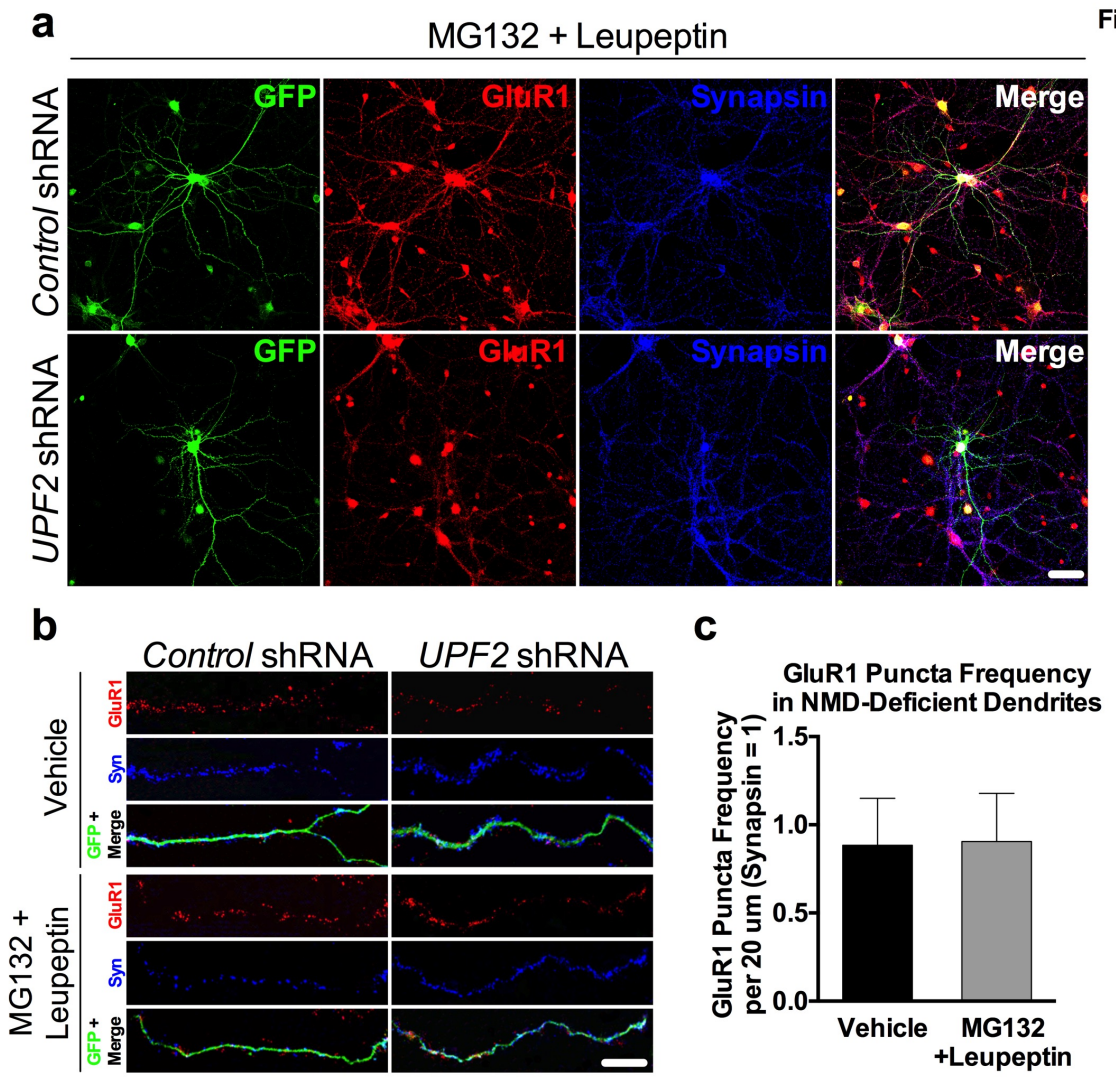
a
MG132 + Leupeptin
Control shRNA
UPF2 shRNA
GFP
GluR1
Synapsin
Merge
b
Control shRNA
UPF2 shRNA
Vehicle
MG132 + Leupeptin
GluR1
Syn
GFP + Merge
c
GluR1 Puncta Frequency in NMD-Deficient Dendrites
GluR1 Puncta Frequency per 20 um (Synapsin = 1)
1.5
1.0
0.5
0.0
Vehicle
MG132 +Leupeptin

Fig. S6 | GluR1 degradation is not altered upon disruption of NMD.
In addition to surface levels (Figure 1), the total expression of local GluR1 in dendrites is also reduced in the absence of NMD (Figure 2**b**). Although the increase in basal internalization rate of GluR1 in the absence of NMD (Figure 2**a**) could account for the reduction in surface levels of this receptor, it does not explain the decrease in total GluR1 levels [7]. Since the disruption of NMD does not alter *GluR1* transcription or degradation (Figure 1), an alteration in the balance of local synthesis and degradation of GluR1 is likely to account for the overall reduction in the total levels of this receptor upon disruption of NMD. Therefore, we examined the local synthesis of nascent GluR1 protein (Figure 3) as well as the degradation of GluR1 upon loss of NMD. Figure 3 shows that the local synthesis of GluR1 is repressed in NMD-deficient dendrites. To study GluR1 protein degradation, we cultured E16 mouse hippocampal neurons in either 24 well plates or in the cell body compartments of tripartite chambers and infected with *UPF2*-shRNA lentivirus at DIV7. In the case of tripartite chambers, we only infected postsynaptic cells with the *UPF2*-shRNA lentivirus. Because endocytosed AMPA receptors can undergo either lysosome- or proteasome-mediated degradation [8-12], we targeted both lysosomal and proteasomal degradation simultaneously. At DIV21, proteasomal and lysosomal degradation were inhibited with 10 μM of the protease inhibitor MG132 and 20 μM of leupeptin, respectively, for 6 hr. For the tripartite experiment, proteasomal and lysosomal degradation were inhibited by treating the synaptic channels with 10 μM of the protease inhibitor MG132 and 20 μM of leupeptin, respectively, for 6 hr. To label surface GluR1, neurons were fixed and stained with an anti-Nterminus-GluR1 antibody without permeabilization (see also extended experimental procedures).
a-b, Representative low (regular cultures) and high magnification (in tripartite chambers) images of GluR1 surface expression in treated and non-treated NMD-deficient dendrites.
c, Quantification of surface GluR1 puncta shows that inhibition of proteasomal and lysosomal degradation did not significantly influence GluR1 puncta frequency in NMD-deficient dendrites (n=3 biological replicates per group; 11 neurons per group).
Data are represented as mean ± SEM. Scale bar: 20 μm.

Figure S7.

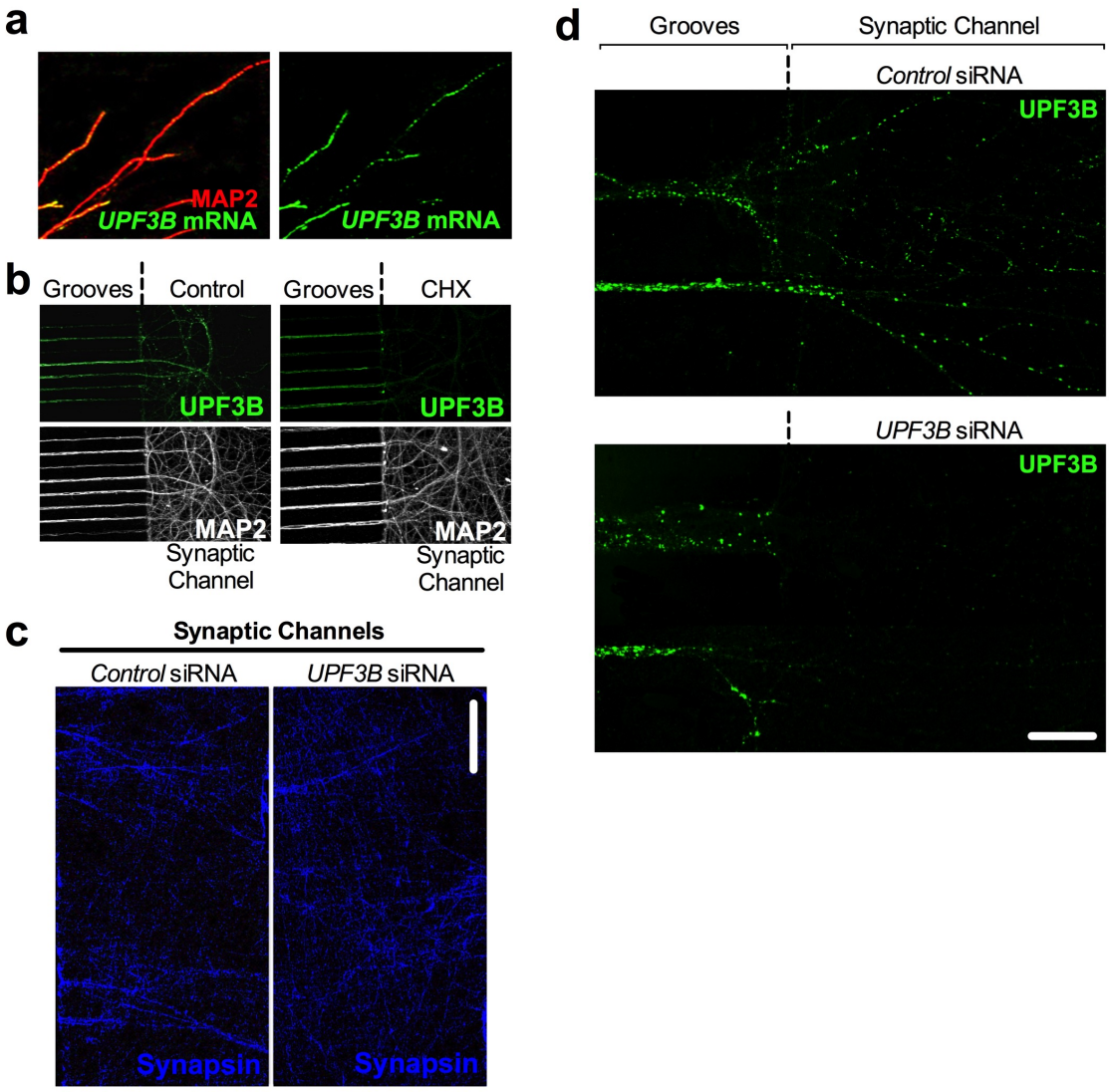
a
MAP2
UPF3B mRNA
UPF3B mRNA
b
Grooves
Control
Grooves
CHX
UPF3B
UPF3B
MAP2
MAP2
Synaptic Channel
Synaptic Channel
c
Synaptic Channels
Control siRNA
UPF3B siRNA
Synapsin
Synapsin
d
Grooves
Synaptic Channel
Control siRNA
UPF3B
UPF3B siRNA
UPF3B

Fig. S7 | UPF3B is locally synthesized in dendrites.
a-b, UPF3B is locally synthesized in hippocampal dendrites. Both dendritic internalization and local synthesis of GluR1 receptor are altered in the absence of NMD. In addition, NMD targets *Arc* and *AMPK* are subjected to translation-dependent degradation in dendrites. Although these data suggest that NMD might regulate GluR1 locally in dendrites, there is no direct evidence for the local requirement for NMD in these compartments.
a, To study the specific requirement of locally-occurring NMD in the regulation of GluR1 within dendrites, we devised a strategy for targeting UPF3B protein (which, like UPF2, is also a specific and major component of the NMD machinery) locally within the synaptic channel of tripartite devices (Figure 4**d**). Dendritic transcriptome analysis showed that the mRNA of UPF3B protein is localized to dendrites [13]. To confirm this, we performed Fluorescent In Situ Hybridization (FISH) on hippocampal neurons with antisense riboprobes against *UP3B* mRNA at DIV21. *UPF3B* FISH resulted in punctate labeling (green) along dendrites confirming the localization of *UPF3B* mRNA to these compartments.
b, Next, we sought to determine if UPF3B is locally synthesized in dendrites. To do this, we inhibited *UPF3B* mRNA translation via dendritic application of Cycloheximide (CHX, 10 μM) and evaluated the UPF3B protein in synaptic channels. We cultured E16 mouse hippocampal neurons in tripartite chambers and, at DIV21, we treated the synaptic channels with CHX for 6 hr. This resulted in an almost complete loss of UPF3B protein in dendrites. MAP2 was used to visualize dendrites in both (**a**) and (**b**).
c-d, To determine whether inhibition of local synthesis of UPF3B in synaptic channels alters GluR1 locally, we selectively treated synaptic channels with siRNAs against the *UPF3B* mRNA and evaluated GluR1 levels (Figure 4**d**). Here, we confirmed that while the treatment of synaptic channels with *UPF3B* siRNA-cocktail (10 nM) for 7 days did not cause an alteration in synaptic potential in these channels (**c**), it led to a complete loss of UPF3B protein (**d**). Note that expression of UPF3B remained intact within dendrites adjacently located within fluidically-isolated microgrooves in panel (**d**).
Data are represented as mean ± SEM. Scale bar: **c** 20 μm, **d** 75 μm.

Figure S8.

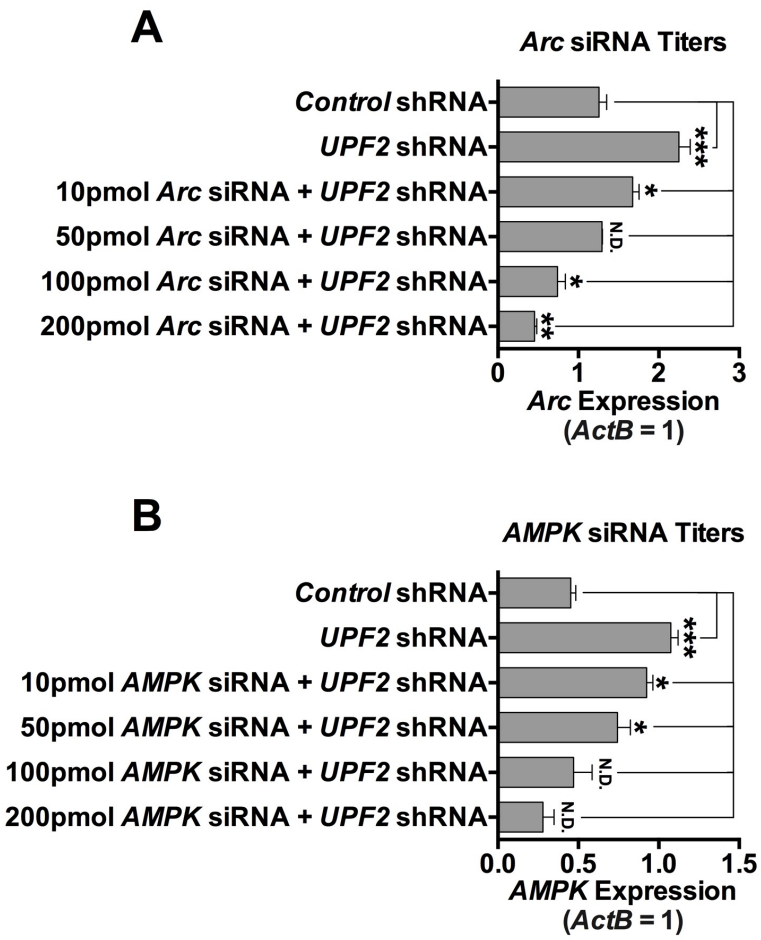
A
Arc siRNA Titers
Control shRNA
UPF2 shRNA
10pmol Arc siRNA + UPF2 shRNA
50pmol Arc siRNA + UPF2 shRNA
100pmol Arc siRNA + UPF2 shRNA
200pmol Arc siRNA + UPF2 shRNA
***
*
N.D.
*
**
0
1
2
3
Arc Expression
(ActB = 1)
B
AMPK siRNA Titers
Control shRNA
UPF2 shRNA
10pmol AMPK siRNA + UPF2 shRNA
50pmol AMPK siRNA + UPF2 shRNA
100pmol AMPK siRNA + UPF2 shRNA
200pmol AMPK siRNA + UPF2 shRNA
***
*
*
N.D.
N.D.
0.0
0.5
1.0
1.5
AMPK Expression
(ActB = 1)

Fig. S8 | *Arc* and *AMPK* titers for siRNA normalization of exaggerated expression in NMD-deficient dendrites.

a-b, We have identified *Arc* and *AMPK* as candidate targets in the NMD-mediated regulation of GluR1 levels within the dendrites and synaptic compartments of hippocampal neurons. We next sought to functionally determine which of these molecules is responsible for depletion of surface GluR1 in NMD-deficient dendrites. To do this, we systematically modulated the elevated levels of *Arc* and *AMPK* in dendrites by siRNA transfection of synaptic channels that contain NMD-deficient dendrites (Figure 6). As siRNA treatment affects mRNA expression in a concentration-dependent manner [14-17], we first determined the amount of siRNA required to correct the levels of each target in NMD-deficient dendrites presented in Figure 6. First, we applied the *UPF2*-shRNA virus to the postsynaptic-cell channels of tripartite microfluidic devices at DIV7. Starting at DIV14, we treated the synaptic channels of NMD-deficient dendrites with non-overlapping siRNAs (2 independent siRNAs per mRNA; see Extended Experimental Procedures) at different concentrations for either *Arc* (**a**) or *AMPK* (**b**). To deliver siRNAs, we used 10% NeuroPORTER (Sigma). At the end of the treatment, synaptic channels were perfused with TRIzol and lysates used for quantitation of *Arc* and *AMPK* mRNA by qRT-PCR. A panel of *Arc* or *AMPK* siRNA-cocktail titers was selectively applied to the synaptic channels of tripartite chambers (n=3 replicates per mRNA and group). As expected, infection of neurons with *UPF2*-shRNA virus significantly increased the expression of *Arc* (**a**) and *AMPK* (**b**).

a, Subsequent treatment with *Arc* siRNA cocktail at 10 pmol led to a significant decrease in the expression of *Arc* mRNA in the dendrites of NMD-deficient postsynaptic neurons, but was still elevated relative to levels observed in the dendrites of postsynaptic neurons in control cultures. Similarly, 100 pmol and 200 pmol titers of *Arc* siRNA cocktail led to a significant downregulation of *Arc* mRNA in the dendrites of NMD-deficient postsynaptic neurons, but produced expression levels lower than that required to recapitulate the physiological profile of dendritic *Arc* mRNA expression observed in control cultures. However, we observed that 50 pmol of *Arc* siRNA cocktail normalized the expression of *Arc* mRNA in the dendrites of NMD-deficient postsynaptic neurons, and that these cultures were indistinguishable from control cultures, leading us to adapt this titer in experiments Figure 6.

b, Treatment of the synaptic channels of tripartite chambers with 10 pmol and 50 pmol titers of *AMPK* siRNA cocktail significantly reduced the overexpression of *AMPK* in the dendrites of NMD-deficient postsynaptic neurons, but did not restore expression levels to those observed in control cultures. 100 pmol *AMPK* siRNA cocktail titer was chosen for functional experiments in Figure 6, as raw values closely resembled and statistically did not differ from those observed in the control group (n=3 replicates).

Data are represented as mean ± SEM; * $p < 0.05$, ** $p < 0.01$, *** $p < 0.001$, N.D. indicates “No Difference”.

Figure S9.

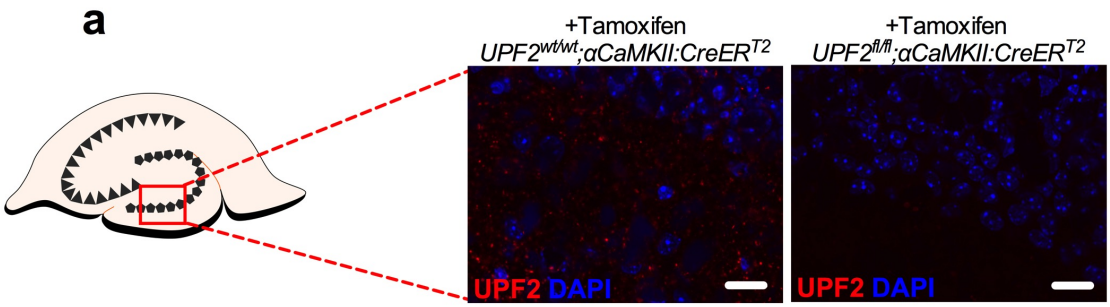
a
+Tamoxifen
UPF2wt/wt;αCaMKII:CreERT2
+Tamoxifen
UPF2fl/fl;αCaMKII:CreERT2
UPF2 DAPI
UPF2 DAPI

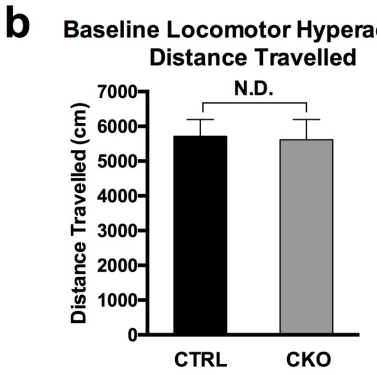
b
Baseline Locomotor Hyperactivity
Distance Travelled
Distance Travelled (cm)
7000
6000
5000
4000
3000
2000
1000
0
N.D.
CTRL
CKO

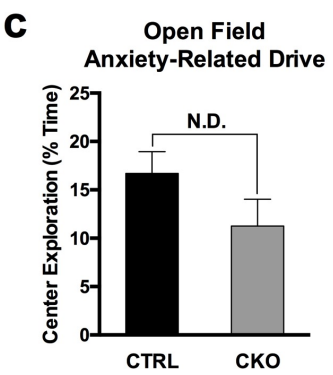
c
Open Field
Anxiety-Related Drive
Center Exploration (% Time)
25
20
15
10
5
0
N.D.
CTRL
CKO

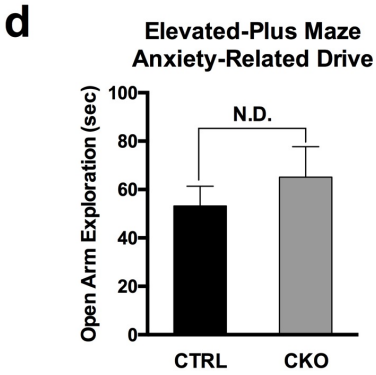
d
Elevated-Plus Maze
Anxiety-Related Drive
Open Arm Exploration (sec)
100
80
60
40
20
0
N.D.
CTRL
CKO

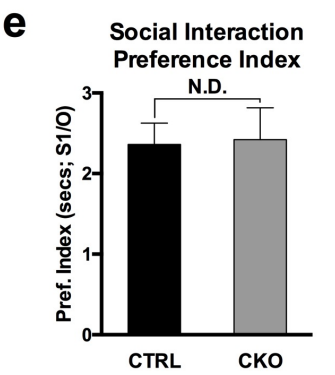
e
Social Interaction
Preference Index
Pref. Index (secs; S1/O)
3
2
1
0
N.D.
CTRL
CKO

Fig. S9 | NMD does not influence baseline locomotor activity, anxiety-related behavior or sociability in mice.

a, NMD regulates GluR1 levels (Figures 1, 2, 3, & S2) which is tightly linked to synaptic plasticity, cognitive function and sociability. However, the extent to which NMD is physiologically relevant to plasticity and behavior is not clear. To determine the potential role of NMD in hippocampus-dependent cognition in the adult brain, we genetically ablated NMD in postmitotic neurons using a conditional knockout mouse of *UPF2* (*UPF2*$^{fl/fl}$) [3]. To temporally control NMD ablation, we crossed *UPF2*$^{fl/fl}$ mice with a mouse line that expresses tamoxifen-inducible Cre under the α*CaMKII* promoter (α*CaMKII*::*CreER*^{T2}) [18]. Before assessing synaptic plasticity (Figure 7), and learning and memory (Figure 8) in *UPF2*$^{fl/fl}$;α*CaMKII*:*CreER*^{T2} (CKO) and *UPF2*$^{wt/wt}$;α*CaMKII*:*CreER*^{T2} (CTRL) mice, we confirmed that conditional deletion of *UPF2* gene (using 200 mg/kg Tamoxifen, for 5 doses) led to the successful loss of UPF2 protein in the hippocampus.

b-d, To determine whether NMD induces hyperactivity, mice were subjected to a 2 hr locomotor hyperactivity assay in photocells. During this 2 hr trial, the distance that mice travelled in cm was analyzed. Greater distances travelled are used as an indicator of locomotor hyperactivity, which may confound behavioral testing on other maze tasks. Similarly, this assay can also assess hypoactivity induced by genetic alterations, which may also influence task performance.

b, In our assessment of baseline locomotor activity, there were no genotype differences between CTRL (n=25) and CKO (n=22) mice. This indicates that loss of NMD does not result in acquired hyper- or hypoactivity.

c, A 10 min open field assay was also conducted in locomotor photocells as an additional control assay, with less time spent exploring the center field of photocells being interpreted as an anxiety-like phenotype. Consistent with the outcome of the locomotor activity assay, no evidence of anxiety-like behavior between CTRL (n=25) and CKO (n=22) mice emerged on this test, indicating that NMD does not modify anxiety-related behavior.

d, The elevated-plus maze was used as a control assay to ensure that NMD did not modify anxiety-related exploratory drive, which may compound measurements of learning and memory. Briefly, mice were subjected to a 10 min test session, with time spent exploring the open arms being used as an index of anxiety-like behavior. No genotype differences emerged between CTRL (n=25) and CKO (n=22) mice on this test.

e, Alterations in both spine density and GluR1 levels are linked to deficits in sociability [19, 20]. In addition, defects in the NMD machinery are linked to numerous neurodevelopmental diseases associated with alterations in normal social behavior [21-26]. To determine whether NMD is required for sociability, we used the three-chamber social interaction task and measured sociability in CTRL and CKO mice. Mice were habituated to the empty three-chamber apparatus for 10 min before being exposed to a stranger mouse placed inside a cup in one chamber and an empty cup in the opposite chamber for an additional 5 min. A preference index was derived from time spent sniffing or interacting with the cup containing the stranger mouse divided by time spent interacting with the empty cup, with higher preference indexes representing more social behavior. No significant differences in preference index emerged between CTRL (n=24)

and CKO (n=19) mice on the three-chamber social interaction assay.
Data are represented as mean ± SEM; N.D. represents “No Difference”. Scale bar: 15 μm.

Figure S10.

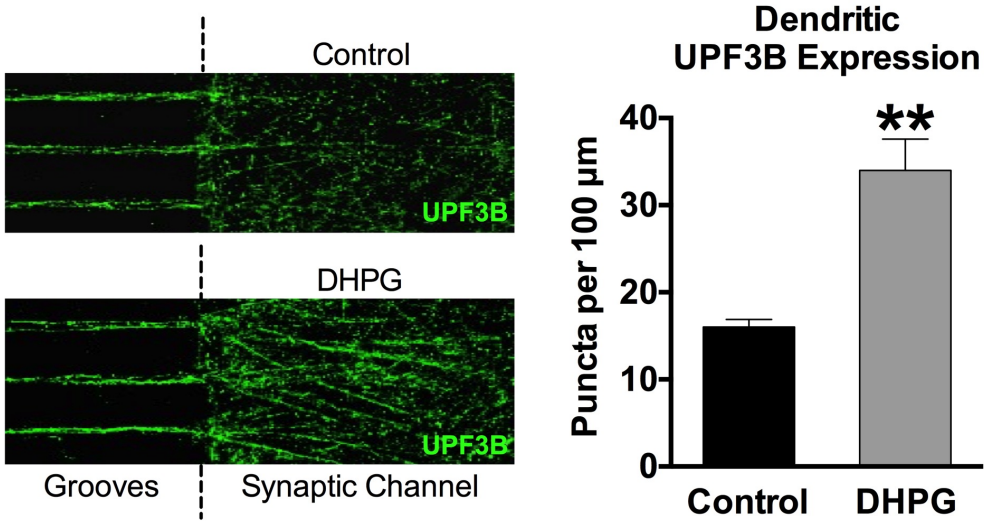
Control
UPF3B
DHPG
UPF3B
Grooves
Synaptic Channel
Dendritic
UPF3B Expression
Puncta per 100 µm
40
30
20
10
0
**
Control
DHPG

Fig. S10 | Neuronal activity upregulates local UPF3B expression in dendrites. The mRNA of UPF3 protein is trafficked to [13] and locally translated in dendrites (see Figure S7). Local translation of selected mRNAs is induced by activity in dendrites [27], suggesting that NMD might be regulated at the level of translation in these compartments. To test this, we stimulated synapses with the mGluR agonist DHPG and measured the levels of UF3B in dendrites. E16 mouse hippocampal neurons were cultured in tripartite microfluidic devices and, at DIV21, the mGluR agonist DHPG (100 μM) was selectively applied to synaptic channels for 5 min to induce synaptic activity. Following fixation of cells, immunostaining for UPF3B was performed in control (vehicle) and DHPG-treated dendrites. Quantification of UPF3B puncta within 100 μm dendrite segments revealed a significant increase in UPF3B expression following treatment with DHPG relative to vehicle-treated cultures (n=3 biological replicates per group). This suggests that NMD is induced by neuronal activity in dendrites.
Data are represented as mean ± SEM; ** $p < 0.01$.

Supplementary References

1. Kim, Y.K., et al., *Mammalian Staufen1 recruits Upf1 to specific mRNA 3' UTRs so as to elicit mRNA decay.* Cell, 2005. **120**(2): p. 195-208.
2. Colak, D., et al., *Regulation of axon guidance by compartmentalized nonsense-mediated mRNA decay.* Cell, 2013. **153**(6): p. 1252-65.
3. Weischenfeldt, J., et al., *NMD is essential for hematopoietic stem and progenitor cells and for eliminating by-products of programmed DNA rearrangements.* Genes Dev, 2008. **22**(10): p. 1381-96.
4. Zheng, S., et al., *PSD-95 is post-transcriptionally repressed during early neural development by PTBP1 and PTBP2.* Nat Neurosci, 2012. **15**(3): p. 381-8, S1.
5. Anggono, V. and R.L. Huganir, *Regulation of AMPA receptor trafficking and synaptic plasticity.* Curr Opin Neurobiol, 2012. **22**(3): p. 461-9.
6. Giorgi, C., et al., *The EJC factor eIF4AIII modulates synaptic strength and neuronal protein expression.* Cell, 2007. **130**(1): p. 179-91.
7. Rial Verde, E.M., et al., *Increased expression of the immediate-early gene arc/arg3.1 reduces AMPA receptor-mediated synaptic transmission.* Neuron, 2006. **52**(3): p. 461-74.
8. Ehlers, M.D., *Reinsertion or degradation of AMPA receptors determined by activity-dependent endocytic sorting.* Neuron, 2000. **28**(2): p. 511-25.
9. Patrick, G.N., et al., *Ubiquitin-mediated proteasome activity is required for agonist-induced endocytosis of GluRs.* Curr Biol, 2003. **13**(23): p. 2073-81.
10. Schwarz, L.A., B.J. Hall, and G.N. Patrick, *Activity-dependent ubiquitination of GluA1 mediates a distinct AMPA receptor endocytosis and sorting pathway.* J Neurosci, 2010. **30**(49): p. 16718-29.
11. Widagdo, J., et al., *Activity-Dependent Ubiquitination of GluA1 and GluA2 Regulates AMPA Receptor Intracellular Sorting and Degradation.* Cell Rep, 2015.
12. Zhang, D., et al., *Na,K-ATPase activity regulates AMPA receptor turnover through proteasome-mediated proteolysis.* J Neurosci, 2009. **29**(14): p. 4498-511.

13. Cajigas, I.J., et al., *The local transcriptome in the synaptic neuropil revealed by deep sequencing and high-resolution imaging.* Neuron, 2012. **74**(3): p. 453-66.
14. Caffrey, D.R., et al., *siRNA off-target effects can be reduced at concentrations that match their individual potency.* PLoS One, 2011. **6**(7): p. e21503.
15. Elbashir, S.M., et al., *Duplexes of 21-nucleotide RNAs mediate RNA interference in cultured mammalian cells.* Nature, 2001. **411**(6836): p. 494-8.
16. Ki, K.H., et al., *The optimal concentration of siRNA for gene silencing in primary cultured astrocytes and microglial cells of rats.* Korean J Anesthesiol, 2010. **59**(6): p. 403-10.
17. Persengiev, S.P., X. Zhu, and M.R. Green, *Nonspecific, concentration-dependent stimulation and repression of mammalian gene expression by small interfering RNAs (siRNAs).* RNA, 2004. **10**(1): p. 12-8.
18. Madisen, L., et al., *A robust and high-throughput Cre reporting and characterization system for the whole mouse brain.* Nat Neurosci, 2010. **13**(1): p. 133-40.
19. Kessels, H.W. and R. Malinow, *Synaptic AMPA receptor plasticity and behavior.* Neuron, 2009. **61**(3): p. 340-50.
20. Penzes, P., et al., *Dendritic spine pathology in neuropsychiatric disorders.* Nat Neurosci, 2011. **14**(3): p. 285-93.
21. Addington, A.M., et al., *A novel frameshift mutation in UPF3B identified in brothers affected with childhood onset schizophrenia and autism spectrum disorders.* Mol Psychiatry, 2011. **16**(3): p. 238-9.
22. Laumonnier, F., et al., *Mutations of the UPF3B gene, which encodes a protein widely expressed in neurons, are associated with nonspecific mental retardation with or without autism.* Mol Psychiatry, 2010. **15**(7): p. 767-76.
23. Lynch, S.A., et al., *Broadening the phenotype associated with mutations in UPF3B: two further cases with renal dysplasia and variable developmental delay.* Eur J Med Genet, 2012. **55**(8-9): p. 476-9.
24. Tarpey, P.S., et al., *Mutations in UPF3B, a member of the nonsense-mediated mRNA decay complex, cause syndromic and nonsyndromic mental retardation.* Nat Genet, 2007. **39**(9): p. 1127-33.
25. Nguyen, L.S., et al., *Contribution of copy number variants involving nonsense-mediated mRNA decay pathway genes to neuro-developmental disorders.* Hum Mol Genet, 2013. **22**(9): p. 1816-25.
26. Xu, X., et al., *Exome sequencing identifies UPF3B as the causative gene for a Chinese non-syndrome mental retardation pedigree.* Clin Genet, 2013. **83**(6): p. 560-4.
27. Wang, D.O., K.C. Martin, and R.S. Zukin, *Spatially restricting gene expression by local translation at synapses.* Trends Neurosci, 2010. **33**(4): p. 173-82.